Title

Mechanisms of cnidocyte development in the moon jellyfish Aurelia

Journal

Evolution & Development, 21(2)

ISSN

1520-541X

Authors

Gold, David A

Lau, Clive Long Fung

Fuong, Holly

et al.

Publication Date

2019-03-01

DOI

10.1111/ede.12278

Peer reviewed

HHS Public Access

Author manuscript

Evol Dev. Author manuscript; available in PMC 2020 May 10.

Published in final edited form as:

Evol Dev. 2019 March ; 21(2): 72–81. doi:10.1111/ede.12278.

Mechanisms of cnidocyte development in the moon jellyfish *Aurelia*

David A. Gold[1,2], **Clive Long Fung Lau**[1], **Holly Fuong**[1,3,4], **Gregory Kao**[1], **Volker Hartenstein**[5], **David K. Jacobs**[1]

[1]Department of Ecology and Evolutionary Biology, University of California, Los Angeles, California

[2]Department of Earth and Planetary Sciences, University of California, Davis, California

[3]Department of Ecology, Evolution, and Environmental Biology, Columbia University, New York, New York

[4]New York Consortium in Evolutionary Primatology, New York, New York

[5]Department of Molecular, Cell, and Developmental Biology, University of California, Los Angeles, California

Abstract

Stinging cells called cnidocytes are a defining trait of the cnidarians (sea anemones, corals, jellyfish, and their relatives). In hydrozoan cnidarians such as Hydra, cnidocytes develop from interstitial stem cells set aside in the ectoderm. It is less clear how cnidocytes develop outside the Hydrozoa, as other cnidarians appear to lack interstitial stem cells. We addressed this question by studying cnidogenesis in the moon jellyfish (Aurelia) through the visualization of minicollagen—a protein associated with cnidocyte development—as well as transmission electron microscopy. We discovered that developing cnidoblasts are rare or absent in feeding structures rich in mature cnidocytes, such as tentacles and lappets. Using transmission electron microscopy, we determined that the progenitors of cnidocytes have traits consistent with epitheliomuscular cells. Our data suggests a dynamic where cnidocytes develop at high concentrations in the epithelium of more proximal regions, and subsequently migrate to more distal regions where they exhibit high usage and turnover. Similar to some anthozoans, cnidocytes in Aurelia do not appear to be generated by interstitial stem cells; instead, epitheliomuscular cells appear to be the progenitor cell type. This observation polarizes the evolution of cnidogenesis, and raises the question of how interstitial stem cells came to regulate cnidogenesis in hydrozoans.

Correspondence: David A. Gold and David K. Jacobs, Department of Ecology and Evolutionary Biology. University of California, Los Angeles. Los Angeles, CA 90095. dgold@ucdavis.edu (D.A.G.); djacobs@ucla.edu (D.K.J.).

AUTHORS' CONTRIBUTIONS

D.A.G. and D.K.J. conceived the project. D.A.G., C.L.F.L., H.F., and G.K. performed the experiments. D.A.G., V.H., and D.K.J. interpreted the data. D.A.G. drafted the manuscript; all authors reviewed and approved the final manuscript.

CONFLICT OF INTEREST

The authors declare no financial or commercial interests, including any corporate funding or affiliations.

SUPPORTING INFORMATION

Additional supporting information may be found online in the Supporting Information section at the end of the article.

1 | INTRODUCTION

Cnidocyte "stinging" cells are an evolutionary novelty that defines the Cnidaria, a clade encompassing sea anemones, corals, jellyfish, and hydroids (Figure 1a). Each cnidocyte contains a large organelle (called a cnida or cnidocyst), which encapsules a coiled thread that is often barbed and associated with toxins. Cnidocytes vary in morphology, and serve specialized functions related to prey capture and defense. As one of the more complex cell-types in the animal kingdom, cnidocytes have been broadly studied to understand their physiology, toxicity, and genetic regulation (Babonis & Martindale, 2014).

Despite this interest, cnidocyte development (also known as cnidogenesis or nematogenesis) has been poorly studied across diverse cnidarians, which hinders our understanding of its evolution. In the model organism *Hydra*, cnidocytes are derived from interstitial stem cells, or "ISCs," which are embedded in the ectoderm and generate most cell types. Cnidogenesis driven by ISC differentiation has been observed in other hydrozoans, and appears to be conserved across this clade (Boelsterli, 1977; Denker, Manuel, Leclère, Le Guyader, & Rabet, 2008). However, non-hydrozoan cnidarians such as sea anemones, corals, box jellies, and scyphozoan jellyfish appear to lack ISCs (Gold & Jacobs, 2013), suggesting that cnidocytes differentiate from some other cell type.

Gold and Jacobs (2013) hypothesized that cnidocytes in scyphozoans might derive from ectodermal epitheliomuscular cells, similar to what is seen in anthozoans such as *Nematostella* (Figure 1a; Zenkert, Takahashi, Diesner, & Özbek, 2011). Here, we study cnidogenesis in the moon jellyfish *Aurelia* ("sp.1" isolate *sensu* Dawson & Jacobs, 2001) to test this hypothesis. *Aurelia* has a complex life cycle including two "adult" forms—the sedentary polyp and free-swimming medusa (Figure 1b). Despite this complexity, *Aurelia* produces a limited number of cnidocyte types (Figure 1c). There is broad agreement that the genus produces atrichous isorhizas and microbasic heterotrichous euryteles, with some authors arguing for additional types or sub-types (Calder, 1971, 1977; Gold et al., 2015; Spangenberg, 1965). Atrichous isorhizas (or haplonemes) are simpler than euryteles, which are larger and possess spined tubules; it has been hypothesized that isorhizas represent an ancient cnidarian ensnaring device, while euryteles function as an "armor-breaking" weapon that co-evolved with the active hunting behaviors of medusozoans (David et al., 2008). In contrast to the two or three types of cnidocytes described in scyphozoans, more than 20 types have been described in hydrozoans (Fautin, 2009). Thus, assessment of cnidogenesis across a complex life history is relatively tractable in *Aurelia*.

To visualize cnidogenesis, we studied the spatial expression patterns of *minicollagen 1* (*NCol-1*, after Kurz, Holstein, Petri, Engel, & David, 1991). Minicollagens are a cnidarian-specific form of collagen, and are the primary proteins in cnidocyte capsule walls. In Hydra, *NCol-1* mRNA expression is restricted to cnidocyte precursor cells (also called cnidoblasts) that have begun to develop the capsule organelle (Kurz et al., 1991). The NCol-1 proteins aggregate through the covalent linkage of disulfide bonds, creating the capsule wall (Özbek, Balasubramanian, & Holstein, 2009). As the cnidocyte matures, the once soluble NCol-1 proteins become insoluble through disulfide-linkage, hardening the capsule wall and decreasing the efficacy of molecular probes (Adamczyk et al., 2010; Engel et al., 2001).

Thus, *NCol-1* offers an excellent candidate marker for immature cnidoblasts and a valuable tool for studying cnidogenesis.

2 | MATERIALS AND METHODS

2.1 | Animals collection and fixation

Planulae, polyps, strobilae, ephyrae, and medusas of *Aurelia sp.1* were collected from the Cabrillo aquarium (San Pedro, CA) or raised at UCLA. Animals were anesthetized in 7.3% $MgCl_2$ before fixation in 4% formaldehydefor 1 hr atroom temperature.

2.2 | Identification of minicollagen genes and phylogenetic analysis

A single, complete minicollagen mRNA was recovered in our *Aurelia sp.1* transcriptome assembly (Gold et al., 2019). Briefly, cDNA libraries were prepared from six time points across the *Aurelia* life cycle, and sequenced using 300 base pair paired-end reads using a HiSeq 2000. The resulting data was cleaned and assembled using the Trinity software package (Haas et al., 2013). The resulting minicollagen sequence was aligned to additional proteins from NCBI using the program MUSCLE (Edgar, 2004), followed by additional refinement of the alignment by hand (available in Additional File 1) A phylogenetic tree was built using RaxML (Stamatakis, 2014), with an LG substitution model and 100 rapid bootstraps. The minicollagen sequence has been deposited in GenBank with accession number MK060014.

2.3 | Verification of Ncol-1 antibody

As part of this project, we received a polyclonal Ncol-1 antibody generated from *Hydra*, which was kindly provided by Suat Özbeck (Engel et al., 2001). To test the efficacy of this antibody in *Aurelia*, we performed western blot analysis on lysates generated from whole animals, as well as cnidocyte isolates. For “whole animal” samples, five polyps and five ephyrae were collected in a 1.8 ml tube. As much liquid was removed from the tube as possible, and the tissue was homogenized using a motorized pestle. For the isolation of cnidocytes, the same number of animals were collected in a 1.8 ml tube. As much liquid was removed from the tube as possible, and the animals were frozen at −80°C overnight. 1.5 ml of homogenization buffer (50% Percoll, 10% sucrose. 0.003% Triton X–100) was added, and the tissue was homogenized by pipetting through an 18-gauge (40 mm) needle six times. The sample was centrifuged at 7500 rpm for 15 min at 4°C, and the supernatant was discarded. This homogenization/centrifugation process was repeated a second time, and the resulting pellet was washed in a recovery buffer (0.003% Triton X–100 and 10% sucrose in PBS). The pellet was spun down a final time at 7500 rpm for 15 min at 4°C, and then re-suspended in recovery buffer. The presence of cnidocytes was verified using light microscopy.

The “whole animal” and “cnidocyte” samples were solubilized by heating at 95°C for 10 min in sample buffer (200 mM Tris-HCl pH 6.8, 8% SDS, 0.4% bromophenol blue, 40% glycerin, 1 M β-mercaptoethanol). The samples were separated by SDS–PAGE using a 4–20% gradient gel, transferred to nitrocellulose membranes, and blocked for 1 hr with Odyssey TBS blocking buffer (LI-COR). The Ncol1 antibody (1:1000) was incubated

overnight at 4°C, and detected using an IRDye 680LT goat anti-rabbit secondary (LI-COR; 1:5000) on a LI-COR Odyssey Instrument.

2.4 | In situ hybridization and antibody staining

PCR primers were designed to amplify a 631 base pair region of the Ncol-1 mRNA (Forward: CGATCTGTCCAACGCAATGT; Reverse: AAAGACTGAGCAGGGCCTAA). To synthesize riboprobes, additional primers were designed with a T7 binding site (TAATACGACTCACTATA) added to the 5′ end of the forward primer (the sense riboprobe) or the reverse primer (the antisense riboprobe). DIG-labeled riboprobes were produced using the MEGAscript® T7 Transcription Kit (ThermoFisher; cat. # AM1333), combined with the primers described above and *Aurelia* cDNA produced using the SuperScript® III First-Strand Synthesis System (ThermoFisher; cat. # 18080051). In situ hybridization was performed following the protocol described in Nakanishi, Yuan, Hartenstein, and Jacobs (2010). Most life stages were assayed using the NBT/BCIP color reaction described in Nakanishi et al. (2010), but an additional fluorescent in situ hybridization protocol (described in the same reference) was used in the ephyra stage, where the latter protocol is most effective. Primary antibodies used for this study include acetylated tubulin (“Atub”; mouse, 1:1,000, Sigma), tyrosinated tubulin (“Ttub”; mouse, 1:800, Sigma), FMRFamide (“FMRF”; rabbit, 1:500, US Biological), Gonadotropin-releasing hormone (rabbit, 1:500, Sigma), and the polyclonal Ncol-1 antibody (“Ncol-1”; rabbit, 1:500). The GnRH gene (*GnRH1*) does not appear to be present in *Aurelia*, but this particular antibody has been previously shown to cross-react with eurytele capsules in *Aurelia* planula (Yuan, Nakanishi, Jacobs, & Hartenstein, 2008) and medusas (Gold et al., 2015). We subsequently refer to this antibody as a “capsule” (“Cap”) marker in the rest of the text. Following primary antibody staining, animals were washed in PBSTr (PBS plus 0.3% Triton X–100) for 2 hr and blocked in 3% normal goat serum for an hour at room temperature (20–25°C). Secondary antibodies include AlexaFluor 555, AlexaFluor 488, and AlexaFluor 647 (Invitrogen, Thermo Fisher Scientific corporation, Carlsbad, CA). Specimens were incubated with fluorescent dyes together with secondary antibodies overnight at 4°C. The specimens were washed in PBSTr for 2 hr at room temperature (20–25°C) and were mounted in ProLong Gold (Invitrogen). Slides were viewed on a Zeiss LSM 700 Confocal Microscope, and digital stacks were manipulated using ImageJ.

2.5 | Transmission electron microscopy

Animals were relaxed in 7.3% $MgCl_2$ for approximately ten minutes, then immediately fixed in 4% paraformaldehyde and 2.5% glutaraldehyde for 24 hr at 4°C. Following fixation, animals were stained with 1% osmium tetroxide for 1 hr at 4°C. The samples underwent an acetone dehydration series (50%, 70%, 96%, and 100% acetone), followed by an epon series (1:3 epon–acetone, 2:2, 3:1, overnight evaporation to 100%) before being transferred into plastic molds for polymerization at 60°C for 16 hr. The epon blocks were submitted to the UCLA Microscopic Techniques Laboratory for sectioning, and were examined using a JEOL 100CX transmission electron microscope.

3 | RESULTS

3.1 | The *Aurelia* minicollagen is most closely related to Ncol-1

We found a single minicollagen gene in *Aurelia sp.1*, which features the conserved domains found in most other minicollagens (Figure 2a). We similarly found a single minicollagen sequence in two previously published *Aurelia* transcriptomes (Brekhman, Malik, Haas, Sher, & Lotan, 2015; Fuchs et al., 2014). So while most cnidarians have multiple minicollagen genes, it appears that *Aurelia* harbors a single copy. The *Aurelia sp.1* minicollagen protein is 332 amino acids long, and is dominated by a repeating motif of glycine followed by two additional amino acids ("Gly-X-Y"). The Gly-X-Y domain is flanked on both sides by proline-rich (polyproline) domains, followed by cystine-rich domains. The 5′ terminus contains a signal peptide. The Gly-X-Y domain in *Aurelia* is longer than any other minicollagen in the NCBI database. Our phylogenetic analysis suggests that the *Aurelia* minicollagen is part of a clade that includes *minicollagen 1* sequences from medusozoans, as well as *Hydra minicollagens* 7, 11, and 12 (Figure 2b). We therefore have named this gene *AurNcol-1*.

3.2 | *Aurelia* Ncol-1 positive cells can be readily identified by antibody staining or in situ hybridization

Western blotting of the Ncol-1 antibody suggests the AurNcol-1 protein behaves in a similar manner as other cnidarian minicollagens (Figure 3m). Based on the amino acid sequence, the predicted size of an AurNcol-1 protein is ~ 30.2 kilodaltons, although the exact size of minicollagens can be difficult to ascertain due to disulfide linkage within and between chains, as well as posttranslational modifications. Ncol-1 Western blots derived from *Aurelia* cnidocyte capsules demonstrate a major band between 20 and 25 kD, consistent with results from *Nematostella* (Zenkert et al., 2011) as well as recombinant expression of *Hydra* Ncol-1 (Engel et al., 2001). Several additional, higher molecular weight bands also exist, and are brighter in whole-animal lysates compared to isolated cnidocytes. These bands are consistent with the denaturing of a complex featuring three minicollagen-1 proteins fused to a maltose binding protein (Engel et al., 2001; Özbek et al., 2002). These results support the efficacy of the *Hydra* Ncol-1 antibody in *Aurelia*.

Across all life stages, the expression of *AurNcol-1* is discrete and punctate, allowing for the identification of individual cnidoblasts. *AurNcol-1* and "capsule" (i.e., non-specific GnRH) expression can be compared to elucidate cnidogenesis; the markers will co-localize in immature cnidoblasts, while *AurNcol-1* will be lost in mature cnidocytes. The expression patterns are easiest to observe in the planula larva, as it has the smallest number of cells (Figures 3a–3g). In the planula, the *Hydra* Ncol-1 antibody colocalizes with the "capsule"-positive signal that demarcates mature euryteles (Figures 3b–3c), but is also expressed in many additional cells (Figures 3b–3d). Digital longitudinal sections clearly demonstrate that these additional Ncol-1 positive cells lie in the lower ectoderm, underneath mature, "capsule" positive cnidocytes (Figures 3e–3g). This observation—combined with previously published evidence that cell division does not occur in the planula endoderm (Gold, Nakanishi, Hensley, Hartenstein, & Jacobs, 2016)—is consistent with the presence of early cnidoblasts in the lower ectoderm, which mature as they migrate superficially. Fluorescent in

situ hybridization combined with the *Hydra* Ncol-1 antibody is possible in the ephyra, and illustrates the colocalization of mRNA and protein expression (Figures 3i–3l). At high magnification (Figures 3j–3k), the expression of mRNA is often associated with more restricted puncta of the Ncol-1 protein. This is consistent with the hypothesis that Ncol-1 proteins localize to the developing capsule wall during cnidogenesis. The Ncol-1 antibody signal can also be found in regions where mRNA expression is absent, such as the distal regions of ephyral arms (Figure 3l). Together, the riboprobe and antibody support the hypothesis that cnidoblasts develop in the lower ectoderm, and migrate superficially during maturation.

3.3 | Patterns of *AurNcol-1* expression are dynamic across life history

In every life stage, the expression of *AurNcol-1* mRNA is more restricted than the distribution of mature cnidocytes. Our fluorescent in situ hybridization protocol is most effective in the ephyra, but all life stages can be assayed with the NBT/BCIP in situ hybridization color reaction (Figure 4). In young planula larvae, *AurNcol-1* positive cells are concentrated towards the future oral pole (Figure 4a). As the planula develops, these cells initially remain localized to the larval oral pole (Figure 4b) but spread aborally in later stages (Figures 4c and 3a). In the polyp, *AurNcol-1* positive cells are ubiquitous across the body column (Figures 4d–4e and 3c). Such cells are abundant in polyp buds (Figure 4d), but nearly absent in the tentacles (Figure 4E), although occasional *AurNcol-1* positive cells can be identified (Figure 4d). Strong *AurNcol-1* expression across the body column continues through strobilation (Figure 4f), but remains largely absent in the tentacles. In the ephyra (Figure 4g), *AurNcol-1* positive cells are ubiquitous with the exception of the distal portion of the manubrium (mouth), the lappets, and the rhopalia (Figures 4h and 3d–3f). In the medusa (Figures 4i–4k), *AurNcol-1* expression is highest on the exumbrellar surface (Figure 4j) and at the base of the tentacles. Similar to the polyp, *AurNcol-1* positive cells are mostly absent from distal portions of the tentacle, but can be found at low levels in some individuals (Figure 4k). This data suggests that the proximodistal migration of cnidoblasts remains consistent through *Aurelia's* life history.

3.4 | TEM suggests that cnidocytes develop from epitheliomuscular cells

AurNcol-1 expression elucidates the regions where cnidoblasts develop, but it does not clarify what cell type serves as the cnidocyte progenitor. To answer this question, we used transmission electron microscopy to analyze two regions: the oral tentacle of the polyp (Figures 5a–5e), and the proximal portion of the medusa marginal tentacle (Figures 5f–5i). We chose to contrast these regions because the polyp tentacle has almost no *AurNcol-1* expression (Figure 4e), while expression in the medusa marginal tentacle is high (Figure 4j). In addition, both regions were well-characterized at the cellular level in a previous study (Gold et al., 2015). Even after trying multiple fixation protocols, our TEM shows limited ability to differentiate cell membranes, especially in the highly vacuolated endodermal cells. However, the cnidocyst organelles are well preserved in our preparations, providing sufficient data to make several important inferences about cnidogenesis in *Aurelia*.

Firstly, cnidocyst maturity can be distinguished by morphology. The variability in cnidocysts can be readily divided into developmental stages based on previously published descriptions

of cnidogenesis (Holstein, 1981), particularly those produced by Denker et al. (2008; reprinted in Figures 5j–5m). Mature cnidocysts, such as those found in the polyp tentacle (Figures 5a–5e), exhibit a thin and electron dense capsule wall, as well as an electron-translucent matrix that visually contrasts with the cnidocyst tubule (Denker et al., 2008; Holstein, 1981). These features are associated with other structures found in mature cnidocytes, such as the operculum (Figure 5c) and/or cnidocil (Figure 5d). Isorhizas dominate the polyp tentacle (Figures 5b–5d) and are easy to distinguish from rarer euryteles (Figure 5e). In the medusa tentacle, many cnidocysts feature traits consistent with immature cnidoblasts, including an unencysted thread, a thick electron translucent capsule, and an electron dense core (Figures 5g–5h). Our interpretation of the TEM data is consistent with patterns of cnidogenesis inferred by *AurNcol-1* expression (Figures 4e and 4j) as well previously published data on cell division in these structures (Gold et al., 2015).

The second conclusion we make from this data is that the medusa tentacle demonstrates a pattern of cnidogenesis that is similar to *Clytia*, but differentiation is initiated from a different cell type. Morphological similarities allow us to recognize early (Figures 5g and 5j), mid-stage (Figures 5h, 5l–5m), and mature cnidocysts (Figures 5i and 5n). This interpretation suggests that cnidocysts develop in the lower ectoderm and migrate superficially as they mature (similar to what is observed in the planula larva, Figure 5g). However, we find no evidence of cells with a morphology comparable to *Clytia's* interstitial stem cells (Figures 5j–5k), which are the progenitors of that species' cnidoblasts. Instead, cnidocysts in the lower ectoderm are associated with basal processes that appear to connect to myofilaments extending alongside the basal surface of the epidermal layer (Figures 5g–5h; Gold et al., 2015). While our TEM is insufficiently detailed to verify the muscular nature of these processes, comparisons with previous descriptions of the medusa tentacle suggest these are myofibril extensions seen in epitheliomuscular cells (Gold et al., 2015). The TEM data is similarly insufficient to determine whether or not mature cnidocytes lose these basal myofibrils, and subsequently lose contact with the basement membrane. However, previous cell proliferation assays in *Aurelia* suggest that cell division is generally low and diffuse (Gold & Jacobs, 2013; Gold et al., 2015), meaning it is unlikely that the pattern of cnidocyte migration seen in this study could be explained by a "conveyer-belt" mechanism where all cell types are being generated in proximal growth zones and shuttled to distal tissues (one possible exception to this being the medusa marginal tentacle, see Gold et al., 2015). We therefore favor a hypothesis where mature cnidocytes detach from the basement membrane and migrate independent of other cells, although this has yet to be confirmed. Based on this evidence, we have illustrated our hypothesized mechanism of *Aurelia* cnidogenesis in Figure 5o. Despite these caveats, our TEM is sufficient to demonstrate that the cnidocyte progenitors in *Aurelia* are morphologically distinct from the interstitial stem cells found in hydrozoans, and are most likely epitheliomuscular cells.

4 | DISCUSSION

In this study, we identify a minicollagen gene in *Aurelia*, and use it to track cnidoblast development through the life cycle. *Aurelia* appears to have a single minicollagen gene, far fewer than those recovered from other cnidarians (including the degenerate myxozoans). This further supports a general relationship between the number of minicollagens in a taxon

and the diversity of cnidocyte types it produces (David et al., 2008; Shpirer et al., 2014; Zenkert et al., 2011). Combining minicollagen-labeling with TEM, we have produced a model for cnidogenesis in *Aurelia*, where epitheliomuscular cells in the lower ectoderm of more proximal tissues produce cnidoblasts, which during their development migrate to more distal regions of the body (Figure 5o). Although *AurNcol-1*expression is largely absent from the oral tentacles of the polyp, the lappets of the ephyra, and the marginal tentacles of the medusa, these regions contain large numbers of mature cnidocytes, and are the structures most responsible for prey capture (Arai, 2012). Ultimately, our results suggest that cnidoblasts migrate into these distal regions to replace those that have discharged.

Cnidogenesis in *Aurelia* reflects a mosaic of traits found in the better-studied hydrozoans (*Hydra* and its relatives) and anthozoans (sea anemones and corals). Migration of cnidocytes into the tentacles—as observed here in *Aurelia*—is a common principle in hydrozoans (Campbell, 1988). But unlike *Hydra*, limited amounts of cnidogenesis can occur in the *Aurelia* tentacle, and in that respect is more similar to what is found in the sea anemone *Nematostella* (Babonis & Martindale, 2014; Zenkert et al., 2011). However, the site of tentacle cnidogenesis in anthozoans appears evolutionarily labile. For example, Westfall (1966) observed cnidogenesis at the base of the tentacle in the sea anemone *Metridium*. In another anemone (*Haliplanella*) cnidoblasts are observed throughout the feeding tentacles, but are restricted to the tentacle base in specialized “catch” tentacles used for interspecies aggression (Watson & Mariscal, 1983). Another trait that *Aurelia* shares with anthozoans is the generation of cnidoblasts from epithelial cells. In *Nematostella*, minicollagen-positive cells are derived from cuboidal epithelial cells, which also exhibit stem-like behavior in the generation of neurons (Nakanishi, Renfer, Technau, & Rentzsch, 2012; Zenkert et al., 2011). This is consistent with the hypothesis that non-hydrozoan cnidarians rely on epithelial cells (as opposed to interstitial stem cell precursors) to generate novel cell types (Gold & Jacobs, 2013). If scyphozoan and hydrozoan medusas are homologous, as recent gene expression data appears to indicate (Kraus, Fredman, Wang, Khalturin, & Technau, 2015), then the restriction of cnidogenesis to the proximal portion of the medusa tentacle could represent an evolutionary precursor to the more complex “tentacle bulbs” seen in hydromedusa such as *Clytia* (Denker et al., 2008). If this interpretation is correct, then the coordination of cnidogenesis in medusas preceded the regulation of cnidogenesis by interstitial stem cells. How cnidocytes could have come under the regulation of a derived stem cell type would be an important future direction for understanding cnidarian evolution and cell-type differentiation

5 | CONCLUSIONS

Through a combination of minicollagen-labeling and TEM, we have constructed a model for cnidogenesis in *Aurelia*. Cnidoblasts originate from epitheliomuscular cells in the lower ectoderm of proximal tissues. Mature cnidoblasts then migrate into the surficial ectoderm, as well as to distal regions of the body where they exhibit high usage and turnover. Our results suggest that the ordered progression of cnidogenesis, as seen in hydromedusas, predates the regulation of this process through progenitor interstitial stem cells.

Funding information

National Institutes of Health, Grant number: T32HG002536; National Aeronautics and Space Administration, Grant number: NAI: Foundations of Complex Life; California Institute of Technology, Grant number: Cordes Postdoctoral Fellowship

REFERENCES

Adamczyk P, Zenkert C, Balasubramanian PG, Yamada S, Murakoshi S, Sugahara K, … Özbek S (2010). A non-sulfated chondroitin stabilizes membrane tubulation in cnidarian organelles. Journal of Biological Chemistry, 285, 25613–25623. [PubMed: 20538610]

Arai MN (2012). A functional biology of Scyphozoa. Netherlands: Springer Science & Business Media.

Babonis LS, & Martindale MQ (2014). Old cell, new trick? Cnidocytes as a model for the evolution of novelty. Integrative and Comparative Biology, 54, 714–722. [PubMed: 24771087]

Boelsterli U (1977). An electron microscopic study of early developmental stages, myogenesis, oogenesis and cnidogenesis in the anthomedusa, *Podocoryne carnea* M. Sars. Journal of Morphology, 154, 259–289. [PubMed: 21970]

Brekhman V, Malik A, Haas B, Sher N, & Lotan T (2015). Transcriptome profiling of the dynamic life cycle of the scypohozoan jellyfish *Aurelia aurita*. BMC Genomics, 16, 74. [PubMed: 25757467]

Calder DR (1971). Nematocysts of polyps of *Aurelia*, *Chrysaora*, and *Cyanea*, and their utility in identification. Transactions of the American Microscopical Society, 90, 269–274.

Calder DR (1977). Nematocysts of the ephyra stages of Aurelia, Chrysaora, Cyanea, and Rhopilema (Cnidaria, scyphozoa). Transactions of the American Microscopical Society, 96, 13–19.

Campbell RD (1988). Migration of nematocytes in hydrozoans In: Hessinger DA, & Lenhoff HM (Eds.), The biology of nematocysts (pp. 123–142). New York: Academic Press.

David CN, Özbek S, Adamczyk P, Meier S, Pauly B, Chapman J, … Holstein TW (2008). Evolution of complex structures: Minicollagens shape the cnidarian nematocyst. Trends in Genetics, 24, 431–438. [PubMed: 18676050]

Dawson MN, & Jacobs DK (2001). Molecular evidence for cryptic species of Aurelia aurita (Cnidaria, Scyphozoa). Biological Bulletin, 200, 92–96. [PubMed: 11249217]

Denker E, Manuel M, Leclère L, Le Guyader H, & Rabet N (2008). Ordered progression of nematogenesis from stem cells through differentiation stages in the tentacle bulb of Clytia hemisphaerica (Hydrozoa, Cnidaria). Developments in Biologicals, 315, 99–113.

Edgar RC (2004). MUSCLE: multiple sequence alignment with high accuracy and high throughput. Nucleic Acids Research, 32, 1792–1797. [PubMed: 15034147]

Engel U, Pertz O, Fauser C, Engel J, David CN, & Holstein TW (2001). A switch in disulfide linkage during minicollagen assembly in *Hydra* nematocysts. EMBO Journal, 20, 3063–3073. [PubMed: 11406583]

Fautin DG (2009). Structural diversity, systematics, and evolution of cnidae. Toxicon, 54, 1054–1064. [PubMed: 19268491]

Fuchs B, Wang W, Graspeuntner S, Li Y, Insua S, Herbst E-M, … Sommer F (2014). Regulation of polyp-to-jellyfish transition in *Aurelia aurita*. Current Biology, 24, 263–273. [PubMed: 24440392]

Gold DA, & Jacobs DK (2013). Stem cell dynamics in Cnidaria: Are there unifying principles?. Development Genes and Evolution, 223, 53–66. [PubMed: 23179637]

Gold DA, Nakanishi N, Hensley NM, Cozzolino K, Tabatabaee M, Martin M, … Jacobs DK (2015). Structural and developmental disparity in the tentacles of the moon jellyfish *Aurelia sp. 1*. PLoS ONE, 10, e0134741. [PubMed: 26241309]

Gold DA, Nakanishi N, Hensley NM, Hartenstein V, & Jacobs DK (2016). Cell tracking supports secondary gastrulation in the moon jellyfish *Aurelia*. Development Genes and Evolution, 226, 383–387. [PubMed: 27535146]

Gold DA, Katsuki T, Li Y, Yan X, Regulski M, Ibberson D, … Greenspan RJ (2019). The genome of the jellyfish Aurelia and the evolution of animal complexity. Nature ecology & evolution, 3, 96–104. [PubMed: 30510179]

Haas BJ, Papanicolaou A, Yassour M, Grabherr M, Blood PD, Bowden J, … Lieber M (2013). De novo transcript sequence reconstruction from RNA-seq using the Trinity platform for reference generation and analysis. Nature Protocols, 8, 1494–1512. [PubMed: 23845962]

Holstein T (1981). The morphogenesis of nematocytes in *Hydra* and *Forsklia*: an ultrastructural study. Journal of Ultrastructure Research, 75, 276–290. [PubMed: 7277568]

Kraus JE, Fredman D, Wang W, Khalturin K, & Technau U (2015). Adoption of conserved developmental genes in development and origin of the medusa body plan. EvoDevo, 6, 23. [PubMed: 26075050]

Kurz EM, Holstein TW, Petri BM, Engel J, & David CN (1991). Mini-collagens in hydra nematocytes. Journal of Cell Biology, 115, 1159–1169. [PubMed: 1955459]

Nakanishi N, Renfer E, Technau U, & Rentzsch F (2012). Nervous systems of the sea anemone *Nematostella vectensis* are generated by ectoderm and endoderm and shaped by distinct mechanisms. Development, 139, 347–357. [PubMed: 22159579]

Nakanishi N, Yuan D, Hartenstein V, & Jacobs DK (2010). Evolutionary origin of rhopalia: Insights from cellular-level analyses of Otx and POU expression patterns in the developing rhopalial nervous system. Evolution and Development, 12, 404–415. [PubMed: 20618436]

Özbek S, Balasubramanian PG, & Holstein TW (2009). Cnidocyst structure and the biomechanics of discharge. Toxicon, 54, 1038–1045. [PubMed: 19286000]

Özbek S, Pertz O, Schwager M, Lustig A, Holstein T, & Engel J (2002). Structure/Function relationships in the minicollagen of *Hydra* nematocysts. Journal of Biological Chemistry, 277, 49200–49204. [PubMed: 12368276]

Shpirer E, Chang ES, Diamant A, Rubinstein N, Cartwright P, & Huchon D (2014). Diversity and evolution of myxozoan minicollagens and nematogalectins. BMC Evolutionary Biology, 14, 205. [PubMed: 25262812]

Spangenberg DB (1965). A study of strobilation in *Aurelia aurita* under controlled conditions. Journal of Experimental Zoology Part A: Ecological Genetics and Physiology, 160, 1–9.

Stamatakis A (2014). RAxML version 8: a tool for phylogenetic analysis and post-analysis of large phylogenies. Bioinformatics, 30, 1312–1313. [PubMed: 24451623]

Watson GM, & Mariscal RN (1983). Comparative ultrastructure of catch tentacles and feeding tentacles in the sea anemone *Haliplanella*. Tissue and Cell, 15, 939–953. [PubMed: 6141650]

Westfall JA (1966). The differentiation of nematocysts and associated structures in the Cnidaria. Zeitschrift für Zellforschung und mikroskopische Anatomie, 75, 381–403. [PubMed: 4383127]

Yuan D, Nakanishi N, Jacobs DK, & Hartenstein V (2008). Embryonic development and metamorphosis of the scyphozoan *Aurelia*. Development Genes and Evolution, 218, 525–539. [PubMed: 18850238]

Zenkert C, Takahashi T, Diesner M-O, & Özbek S (2011). Morphological and molecular analysis of the *Nematostella vectensis* cnidom. PLoS ONE, 6, e22725. [PubMed: 21829492]

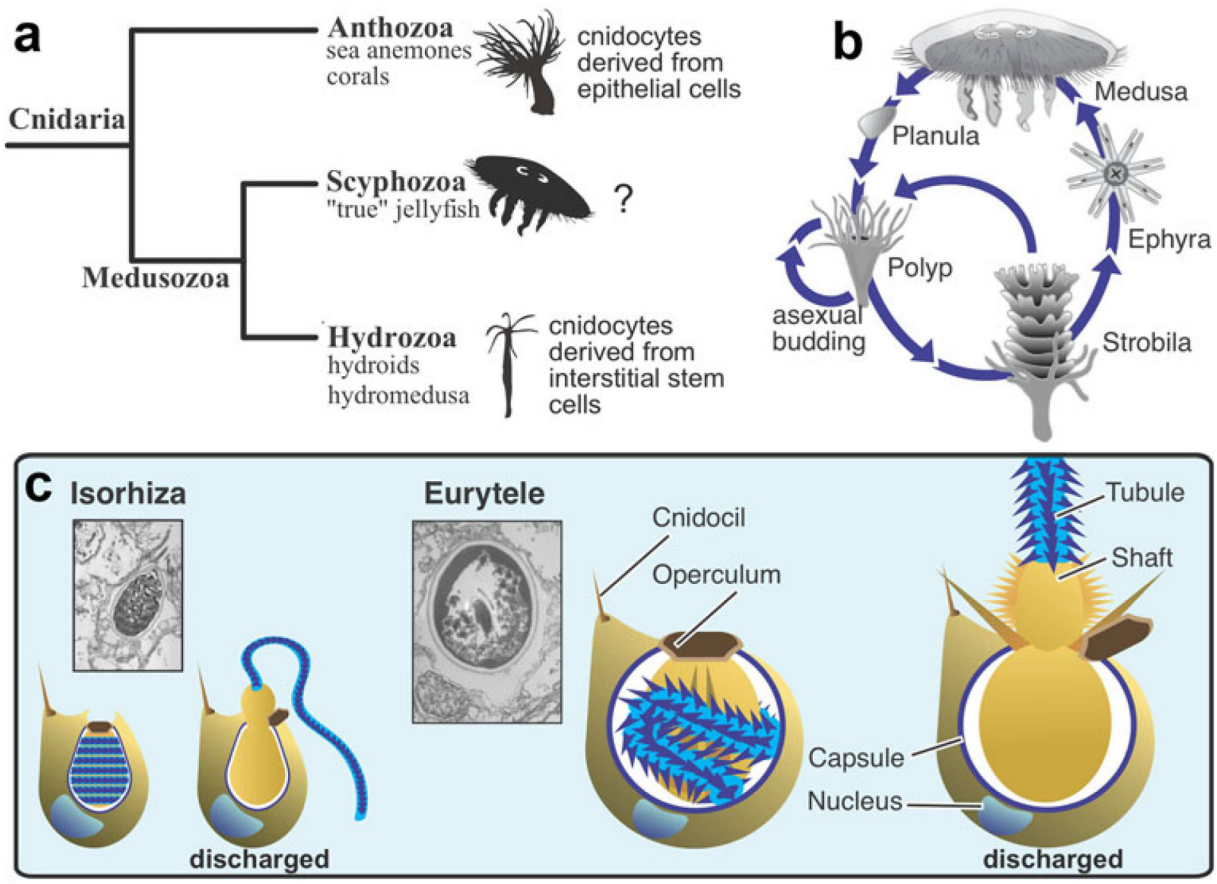

FIGURE 1.

Life cycle and cnidocyte types in Aurelia. (a) A phylogeny of major cnidarian groups discussed in this study. A description of the cnidogenesis is described to the right of each clade. (b) Life cycle of Aurelia, demonstrating the major stages. (c) The two major cnidocyte types described in Aurelia, shown to scale. Left: the isorhiza. Right: the eurytele. For both cnidocyte types, the top image provides a transmission electron microscopy photograph of the cnidocyte. Underneath are illustrations of the cnidocyte undischarged (left) and discharged (right)

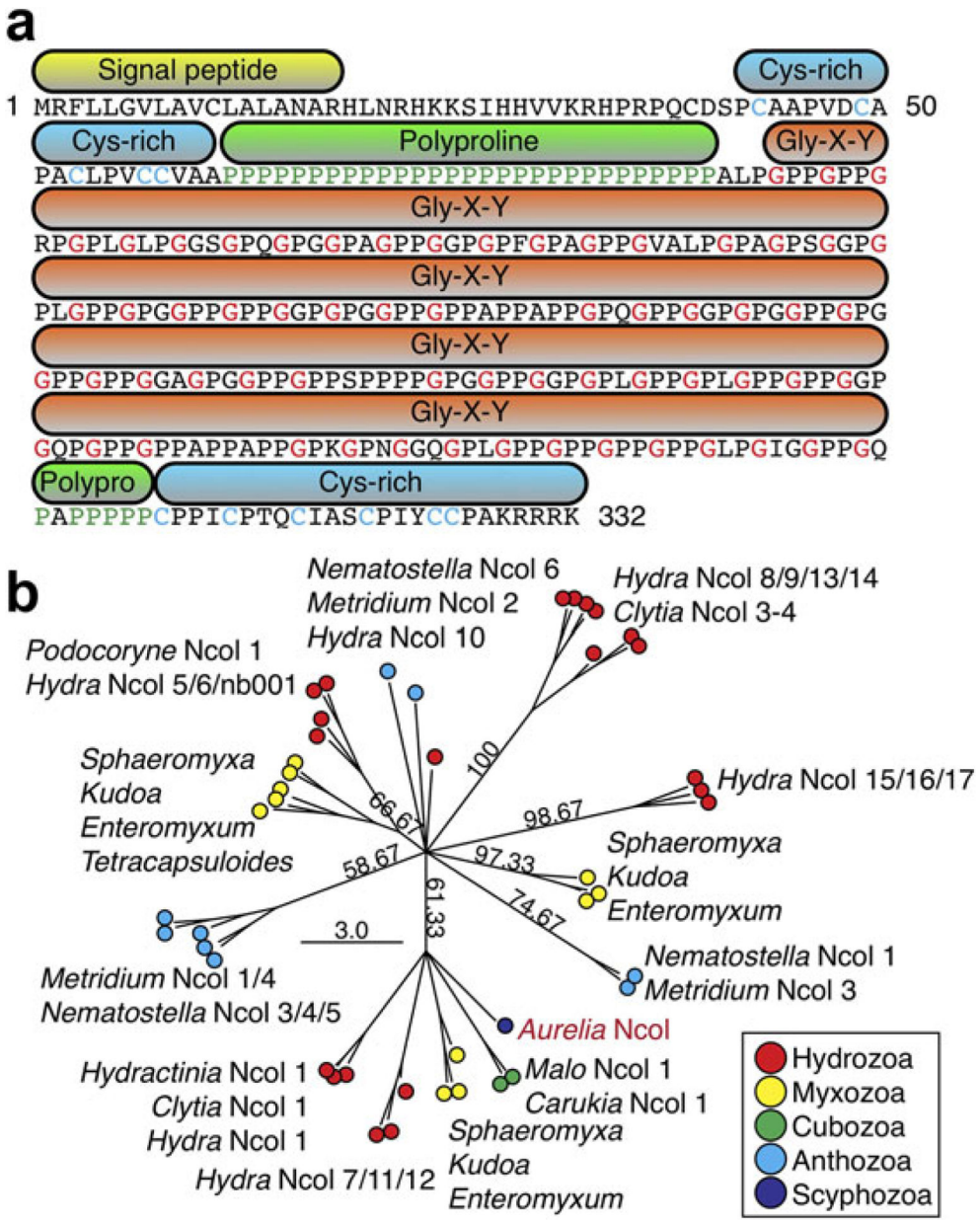

FIGURE 2.

Structure and relationship of the AurNcol-1 gene. (a) Peptide sequence of AurNcol-1, with the conserved domains identified. (b) A maximum likelihood-based phylogenetic tree of cnidarian minicollagens

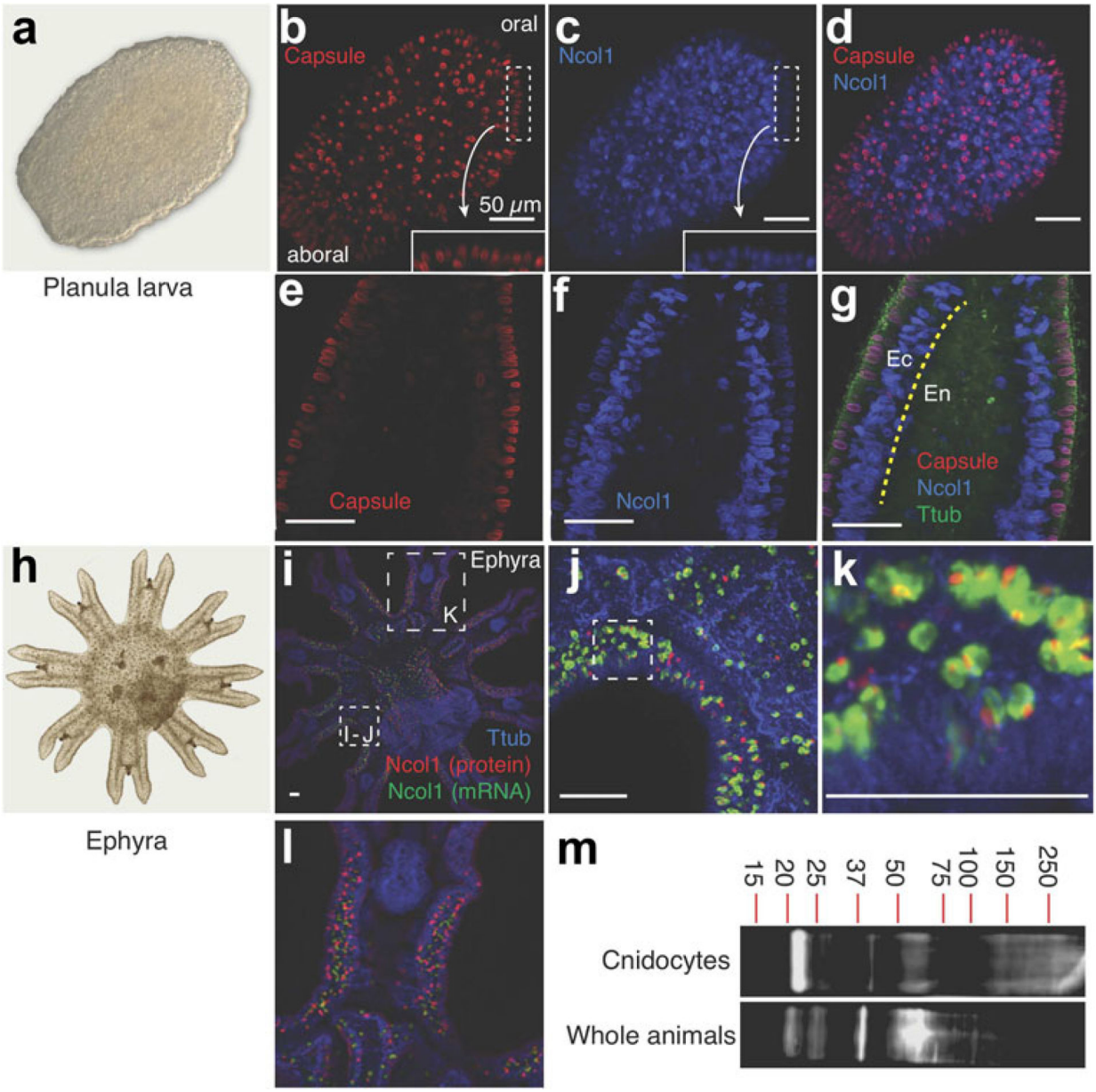

FIGURE 3.

Fluorescent imaging of AurNcol-1 mRNAs and antibodies. (a) A light microscopy image of a planula larvae. (b–d) Coexpression of Hydra Ncol-1 antibody and the eurytele-specific “capsule” antibody in a planula larva. These images demonstrate that Ncol-1 expression overlaps with “capsule”-positive euryteles (e.g., arrows in Figures 3b–3c), but that additional Ncol-1-positive cells lie underneath these cells. (e–g) A digital longitudinal section of another planula. (g) Additional staining with tyrosinated tubulin to differentiate endoderm (En) from ectoderm (Ec). The boundary between the two germ layers is noted on the left side with a yellow line. Note that the Ncol-1 antibody signal is strongest in the lower portion of the ectoderm. (h) A light microscopy image of an ephyra. (i–l) Fluorescent in situ hybridization of the AurNcol-1 mRNA in an ephyra, coexpressed with the Hydra Ncol-1 protein and tyrosinated tubulin. (j) Higher magnification image of (i), focused on the base of

the ephyra's arms. (k) Higher magnification image of the box within (j). Note the common pattern where a puncta of protein expression (red) is colocalized within an mRNA signal (green). (l) Close-up of (i) focusing on the distal region of the ephyra's arm. Note the loss of mRNA signal (green) in more distal cells. (m) Western blots produced from isolated ephyra and polyp cnidocytes (top) as well as ephyra and polyp tissues (bottom)

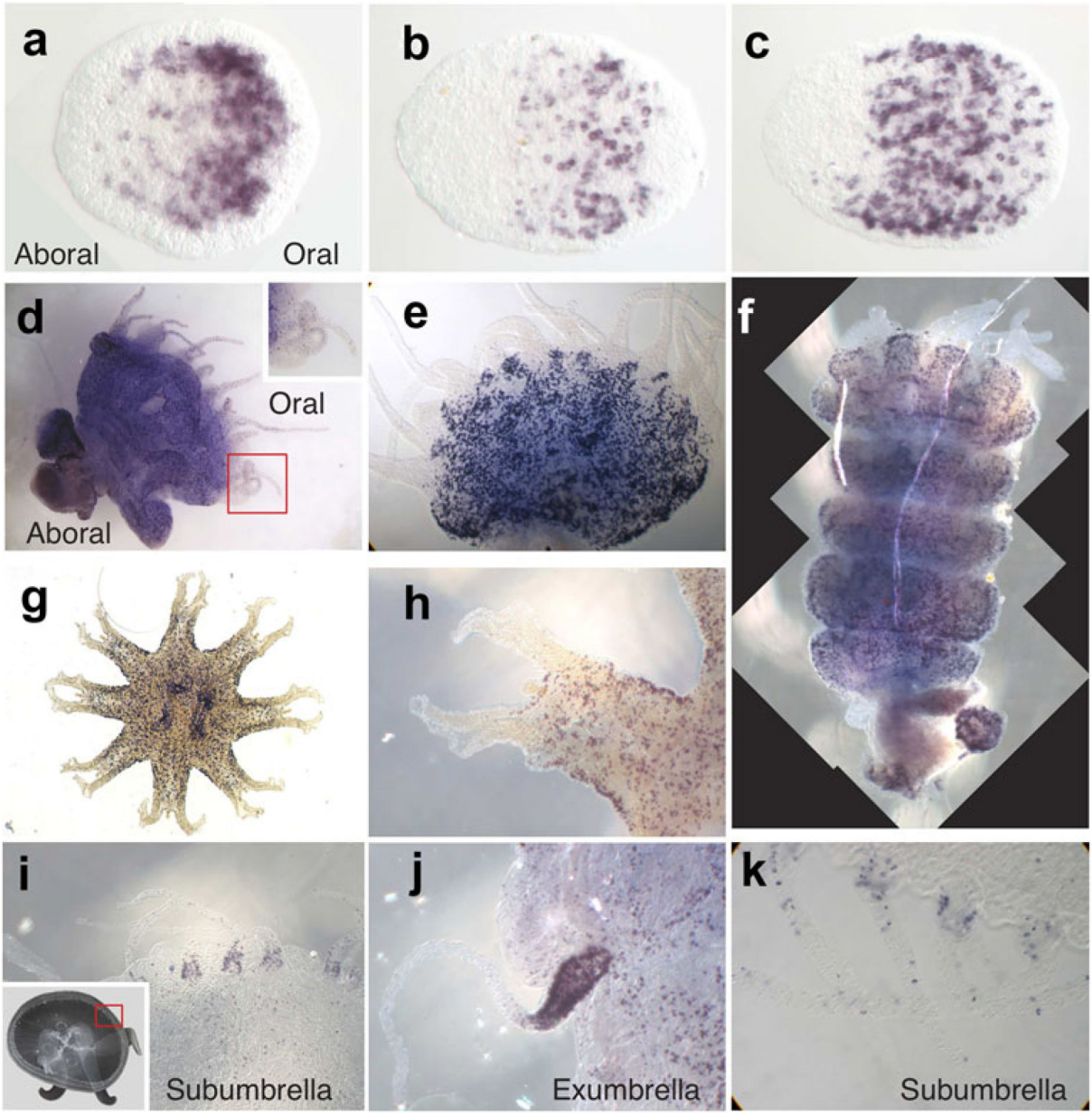

FIGURE 4.

AurNcol-1 expression through the Aurelia life cycle, as revealed by in situ hybridization. (a) Planula larva collected immediately from a brooding female medusa. (b) Planula larva 3 days post-collection. (c) Planula larva 5 days post-collection. (d) A polyp, demonstrating limited AurNcol-1 expression in the distal portions of the tentacle. (e) Close-up of another polyp, where AurNcol-1 expression is absent in the tentacles. (f) A strobila. (g) An ephyra, with the aboral side up. (h) Close-up of an ephyra arm from 4G. (i) The bell margin of a young medusa (approx. 3 cm in diameter) with the subumbellar/oral side facing up. A low-magnification photograph of a medusa is provided in the lower-left insert to provide context; the region under examination in (i) is shown with a red box. (j) A close-up of a single tentacle from a young medusa, with the exumbrellar side facing up. (k) The bell margin of

another medusa, demonstrating limited AurNcol-1 expression in the distal portions of the tentacle

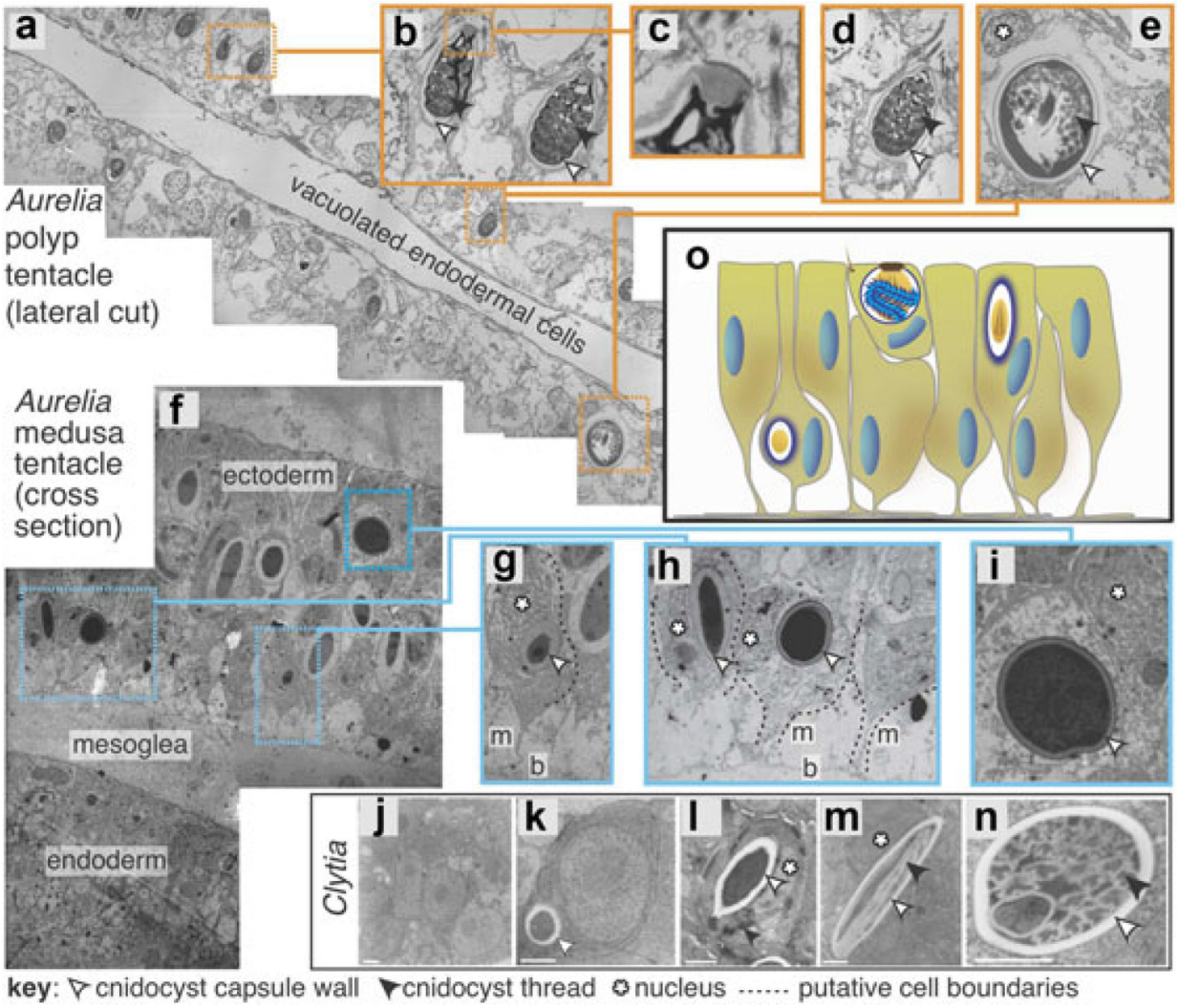

FIGURE 5.

Transmission electron microscopy of cnidogenesis in Aurelia, with a comparison to the hydromedusa Clytia. (a–e) Cnidocyte morphology in the polyp oral tentacle. (a) Longitudinal cut across an polyp tentacle. (b) Several mature isorhizas. (c) A closeup of one isorhizas, showing the detail of the operculum. (d) Another image of a mature isorhiza, demonstrating the presence of a cnidocil. (e) Closeup of a mature eurytele. (f–i) Cnidogenesis in the medusa marginal tentacle. (f) Oblique cut through the medusa tentacle epithelium. (g) A putative epitheliomuscular cell differentiating into a cnidoblast. Putative myofilaments are labeled with an “m”; the basement membrane is labeled with “b.” (h) Several cnidocysts taking on an elongated shape of maturing cnidocysts. Note the displaced nuclei (marked with an asterisk) and associated basal processes. (i) Mature eurytele in the superficial ectoderm. (j–m) Progression of cnidogenesis in the tentacle of Clytia, reprinted from Denker et al. (2008). (j) Interstitial stem cells. (k) A former interstitial stem cell (now a nematoblast) with a developing cnidocyst. (l–n) Developing cnidocysts. (o) Schematic of cnidogenesis based on our interpretation of (f)